Colloid Polym Sci (2008) 286:1123–1133
DOI 10.1007/s00396-008-1874-2

ORIGINAL CONTRIBUTION

Convectional, sedimentation, and drying dissipative patterns of colloidal crystals of poly (methyl methacrylate) spheres on a cover glass

Tsuneo Okubo · Junichi Okamoto · Akira Tsuchida

Received: 21 February 2008 / Accepted: 7 April 2008 / Published online: 25 April 2008

Abstract Direct observation of the convectional dissipative patterns was successful during the course of dryness of colloidal crystals of poly (methyl methacrylate) spheres on a cover glass. Formation processes of the convectional patterns of spoke-like lines were observed as a function of sphere size and also sphere concentration. During dryness of the suspensions, the brilliant iridescent colors changed beautifully. Macro- and microscopic drying patterns and thickness profiles of the dried film were observed. Sharp broad rings were observed especially at low sphere concentrations. The water evaporation accompanied with the convectional flow of water and the colloidal spheres played an important role for these dissipative structure formation.

Keywords Poly (methyl methacrylate) colloids · Convectional pattern · Drying pattern · Dissipative structure · Spoke line · Broad ring · Cover glass

T. Okubo (✉)
Institute for Colloidal Organization,
Hatoyama 3-1-112, Uji,
Kyoto 611-0012, Japan
e-mail: okubotsu@ybb.ne.jp

T. Okubo
Cooperative Research Center, Yamagata University,
Johnan 4-3-16,
Yonezawa 992-8510, Japan

J. Okamoto · A. Tsuchida
Department of Applied Chemistry, Gifu University,
Gifu 501-1193, Japan

Introduction

Most structural patterns in nature are formed via self-organization accompanied with the dissipation of free energy and in the non-equilibrium state. Among several factors in the free-energy dissipation of aqueous colloidal suspensions, evaporation of water molecules at the air–water interface and the gravitational convection are very important. In order to understand the mechanisms of the dissipative self-organization of the simple model systems, instead of much complex nature itself, several research groups including us have studied the *convectional* [1–7], *sedimentation* [8–12], and *drying* dissipative patterns during the course of drying suspensions and also solutions [13–49].

Interestingly, macroscopic *broad ring* drying patterns of the hills accumulated with solutes at the outside edge were formed for almost all solutes. For the non-spherical-shaped solutes, however, a central round hill was formed in the central area in addition to the broad rings. Macroscopic spoke lines, cracks, or fine hills, including flickering spoke lines, were also observed in the dried film for many solutes. Furthermore, so many types of microscopic drying patterns such as branch-, arc-, block-, star-, cross-, string-like, and others were observed. It should be noted here that the macroscopic broad rings and spoke lines were observed already in the convectional and/or sedimentation patterns. The broad ring sedimentation patterns in the liquid phase were observed first in a previous paper from the author's laboratory [9] as the author knows, though the broad ring formation in the dried films has been reported so often. A main cause for the broad ring and spoke lines is due to the convectional flow of water and solutes mainly from the central area toward the outside edge in the upper and/or

lower layers of the liquid, which was observed directly from the movement of the reversibly occurred aggregates of the colloidal particles of Chinese black ink on water surface and in a glass dish [1–3, 6]. Clearly, the convectional flow is enhanced by the evaporation of water at the liquid surface, resulting in the lowering of the suspension and/or solution temperature in the upper region of the liquid. Magnitudes of the temperature lowering at the liquid surface at 25 °C compared with the bulk temperature were estimated to be 2 °C and 1.5 °C at the humidities of air, 40% and 80%, respectively, and those at 40 °C were 5 °C and 2 °C, respectively [49, 50]. It should be mentioned

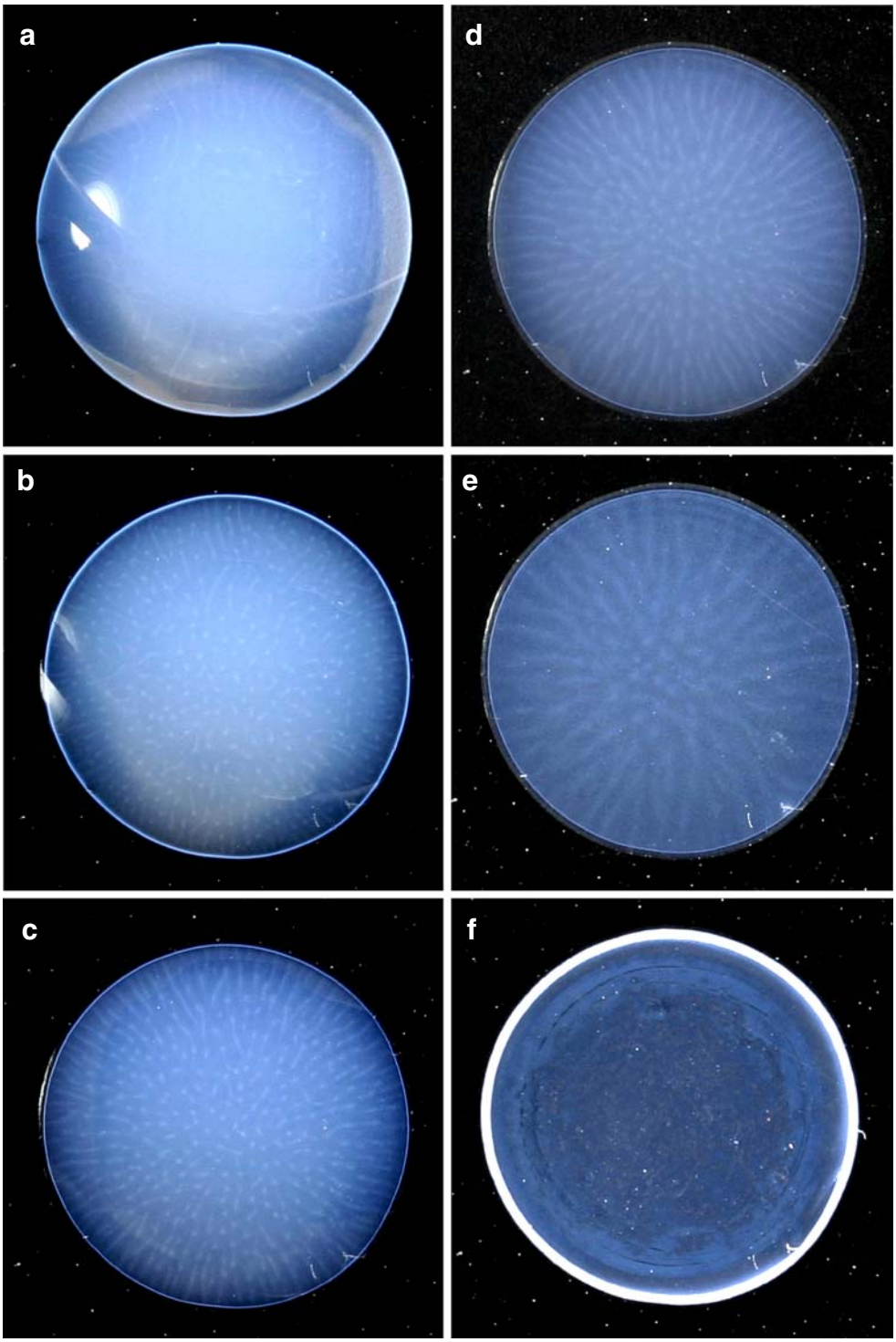

Fig. 1 Convectional patterns of GW1 spheres on a cover glass at 25 °C. ϕ=0.00095. **a** 110 m after setting, **b** 3 h, **c** 3 h, 40 m, **d** 4 h, **e** 4 h, 15 m, **f** 5 h (dry)

further that the vague primitive patterns formed already in the liquid state before dryness, and they grew toward the fine structures during the course of solidification [38]. It should be further mentioned here that the theoretical study for these convectional patterns using Navier–Stokes equations is not always successful [5, 51–55].

In this work, the convectional spoke-line patterns were observed successfully for colloidal crystal suspensions of poly (methyl methacrylate) (PMMA) spheres (100, 200, and 300 nm in diameter). Colloidal surfaces of PMMA spheres are weakly hydrophobic in aqueous suspension. Thus, it is highly plausible that the reversible and temporal aggregates of PMMA spheres are formed, and their convectional flows are visualized as like as Chinese black ink [6]. The other reason why the convectional patterns are visualized for PMMA system will be the partial and local

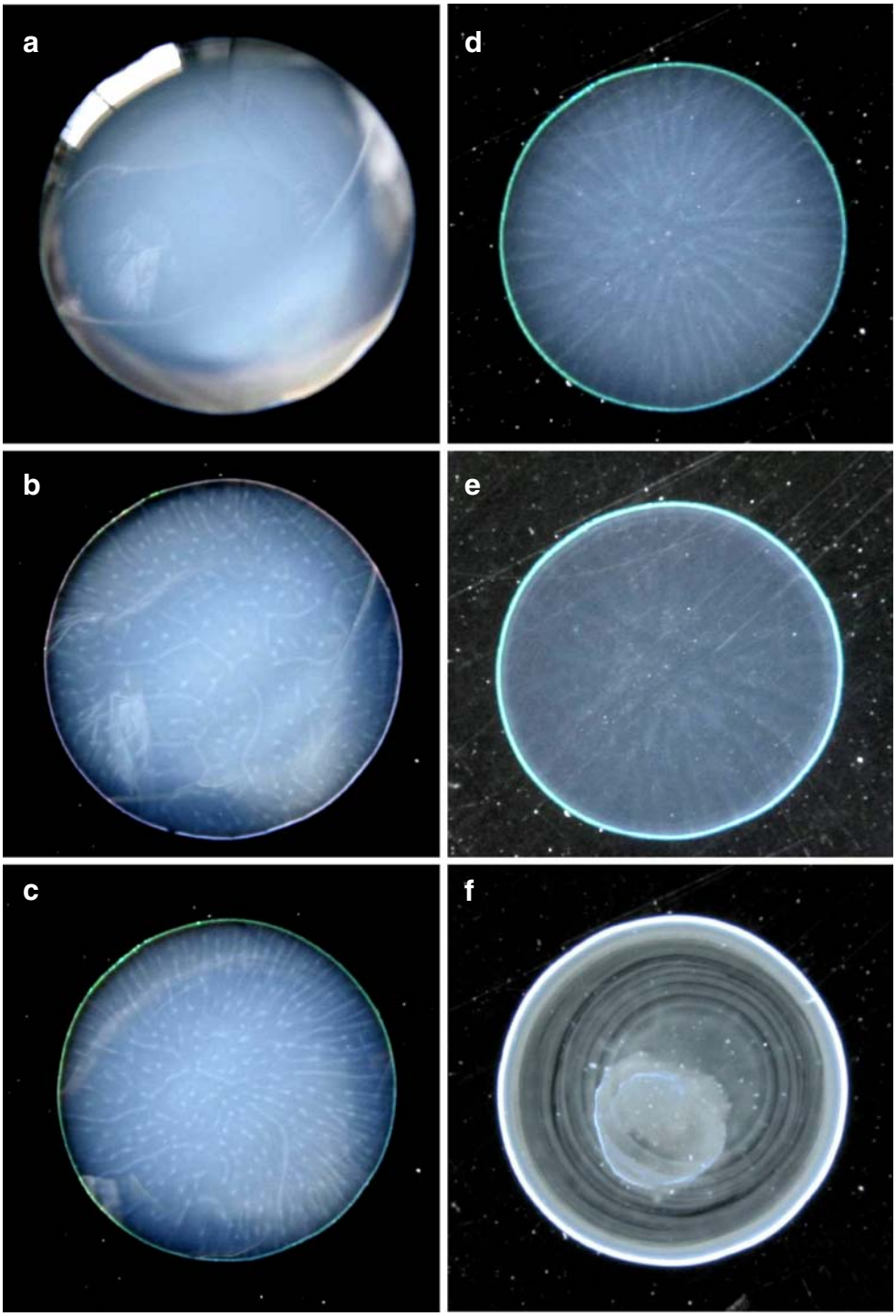

Fig. 2 Convectional patterns of GW6 spheres on a cover glass at 25 °C. ϕ=0.000210. **a** 25 m after setting, **b** 2 h, 20 m, **c** 3 h, 15 m, **d** 4 h, **e** 4 h, 10 m, **f** 4 h, 55 m (dry)

melting of the colloidal crystals of PMMA, especially for the suspensions at higher concentrations than 0.01 in volume fraction. Macro- and microscopic drying patterns of the colloidal crystals of PMMA spheres, their size ranging from 100 nm to 1.0 μm, were also studied in detail in this work.

Experimental

Materials

PMMA spheres, GW1 (100±7 nm in diameter and polydispersity index), GW6 (200±10 nm), GW8 (300±

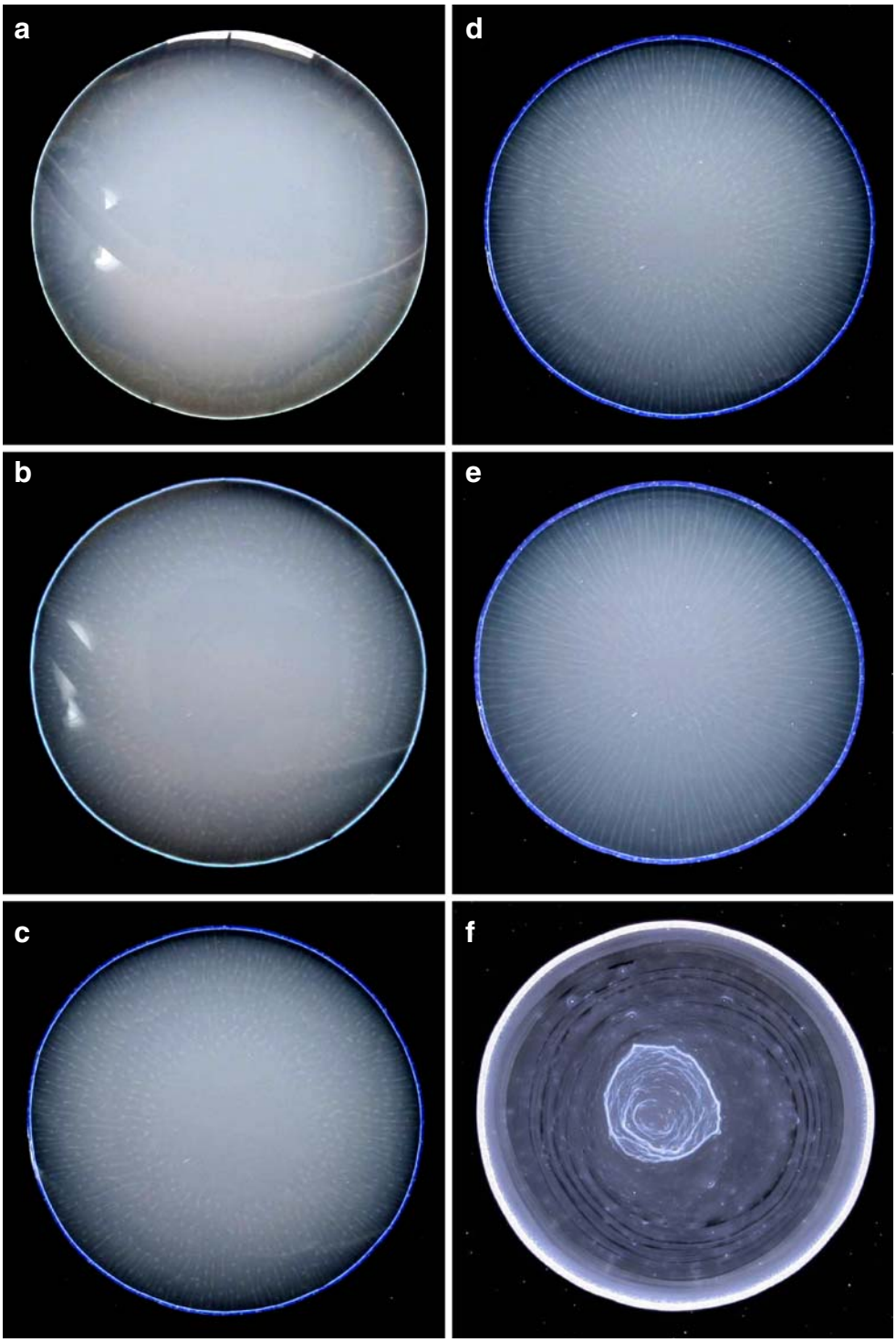

Fig. 3 Convectional patterns of GW8 spheres on a cover glass at 24 °C. ϕ=0.00074. **a** 1 h, 15 m after setting, **b** 2 h, 25 m, **c** 3 h, 20 m, **d** 3 h, 45 m, **e** 4 h, **f** 5 h, 10 m (dry)

12 nm), and PM1000 (1.0 mm±20 nm) were kindly donated by the Soken Chemicals Co. (Tokyo, Japan). These size parameters were determined on an electron microscope. PM1000 spheres were carefully purified more than 30 times by a decantation with pure water since a large amount of the detergents used for sphere synthesis must be deleted from the stock suspension. Then, all the stock sample suspensions were treated on a mixed bed of cation- and anion-exchange resins [Bio-Rad, AG501-X8(D), 20–50 mesh] for more than 4 years before use. The stock suspensions from GW1 to PM1000 spheres thus obtained were crystallized and emitted strong iridescent bluish to whitey colors, respectively. Water used for the sample preparation was purified by a Milli-Q reagent grade system (Milli-RO5 plus and Milli-Q plus, Millipore, Bedford, MA, USA).

Observation of the dissipative structures

Volumes of 0.1 ml of the suspensions were dropped carefully and gently on a micro cover glass (30 mm×30 mm, thickness no. 1, 0.12 to 0.17 mm, Matsunami Glass Co., Kishiwada, Osaka) set in a plastic dish (type NH-52, 52 mm in diameter, 8 mm in depth, As One Co., Tokyo, Japan). The cover glasses were used without further rinse. The contact angle for the pure water was 31±0.5° from the drop profiles of water on the cover glass. Extrapolation to the zero amount of water was made from the measurements at the several amount of water. A disposable serological pipet (1.0 ml, Corning Lab. Sci., Co.) was used for the dropping the suspension on a cover glass. Observation of the macro- and microscopic drying patterns was made for the film formed after the suspension was dried up completely on a cover glass in the temperature-regulated room at 25 °C or 24 °C. Humidity was not regulated and between 50% and 60%. Sphere concentrations were between 0.0002 and 0.08 in volume fraction.

Macroscopic convectional and drying patterns were observed on a Canon EOS 10 D digital camera with a macro-lens (EF 50 mm, f=2.5) and a life-size converter EF. Microscopic drying patterns were observed with a metallurgical microscope (PME-3, Olympus Co., Tokyo, Japan). Thickness profiles of the dried films were measured on a laser 3D profile microscope (type VK-8500, Keyence Co., Osaka, Japan).

Results and discussion

Convectional and sedimentation patterns of PMMA spheres

Figures 1, 2 and 3 show the typical examples of the time change in the convectional patterns of GW1, GW6, and GW8 spheres, respectively. These convectional patterns were not observed clearly with the naked eyes since the patterns were too small to be recognized with the naked eyes. Surprisingly, the convectional patterns were observed in the extended pictures. The convectional patterns, however, were not observed for PA1000 spheres, which will be due to the strong multi-scattering of light. At a first glance, these convectional patterns for the small PMMA spheres are quite similar to those of Chinese black ink [6]. Several important findings are obvious in these figures. Firstly, the few and rather curved spoke lines formed at the outside area of the liquid at the initial state. The lines developed toward central area accompanied with increase in the line number. As Terada et al. [1–3] and the authors [6] observed the convectional patterns of Chinese black ink on water and a glass dish, a large number of the very small convectional circles (*cell convections*) were formed to the normal direction of the spoke lines. It is highly plausible that each spoke line is composed of the valleys and hills with the up- and

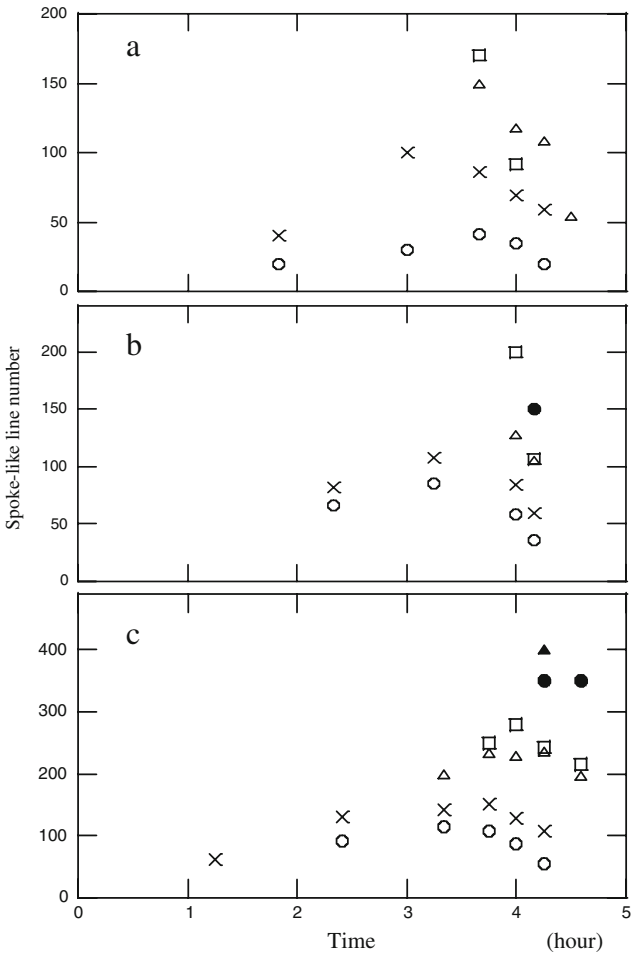

Fig. 4 Change in spoke-like line number of GW1 (**a**), GW6 (**b**), and GW8 (**c**) with time on a cover glass. **a** *Open circles* ϕ=0.000318, *x marks* 0.00095, *open triangles* 0.00318, *open squares* 0.0064. **b** *Open circles* ϕ=0.000210, *x marks* 0.00063, *open triangles* 0.00210, *open squares* 0.00420, *closed circles* 0.0105. **c** *Open circles* ϕ=0.000245, *x marks* 0.00074, *open triangles* 0.00245, *open squares* 0.00490, *closed circles* 0.0123, *closed triangles* 0.0245

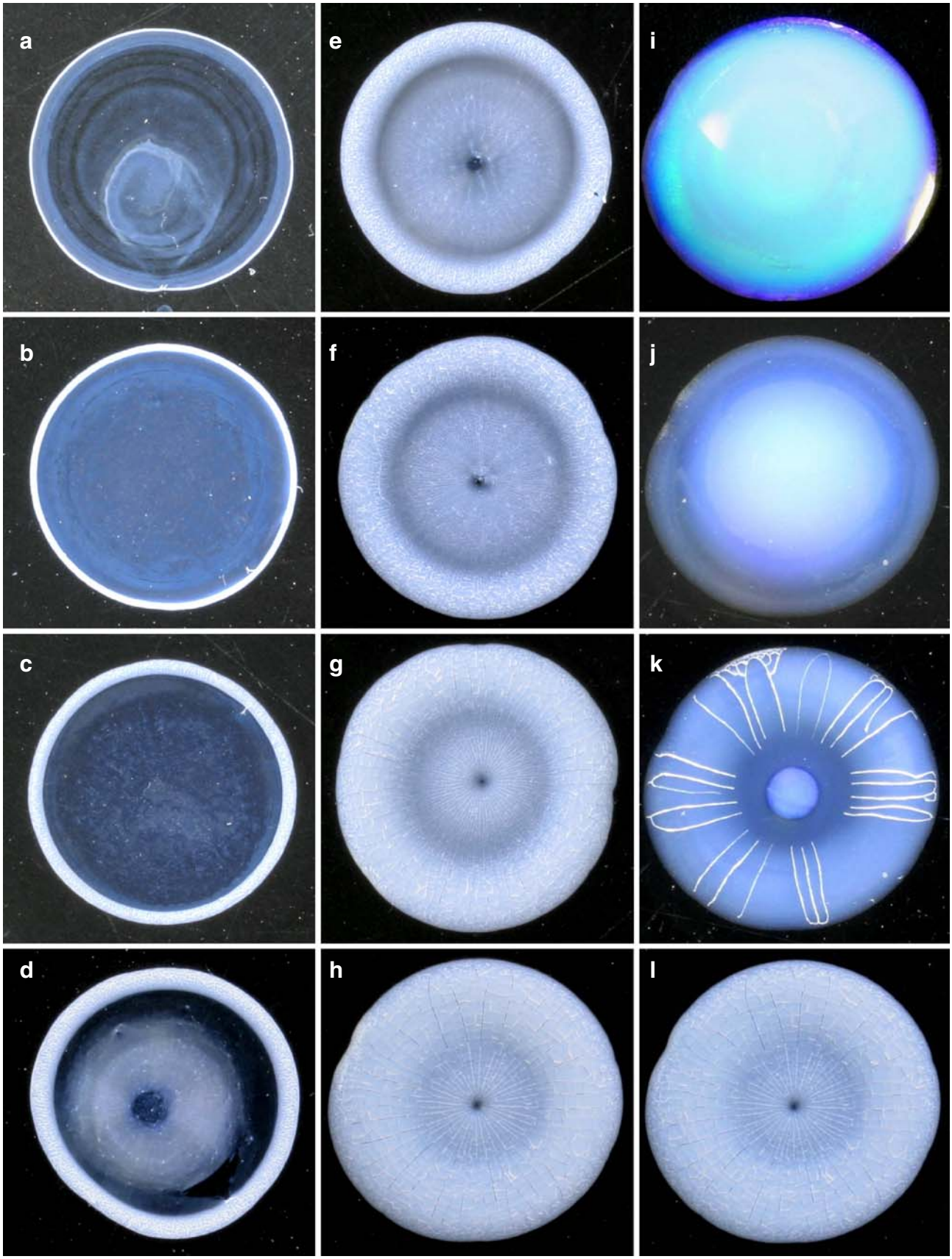

Fig. 5 Drying patterns and change of patterns during dryness of GW1 spheres on a cover glass at 25 °C. **a** ϕ=0.000318, **b** 0.00095, **c** 0.00318, **d** 0.0064, **e** 0.0159, **f** 0.021, **g** 0.064, **h** 0.095, **i** ϕ=0.095, 30 m after setting, **j** 3 h, **k** 3 h, 40 m, **l** 4 h

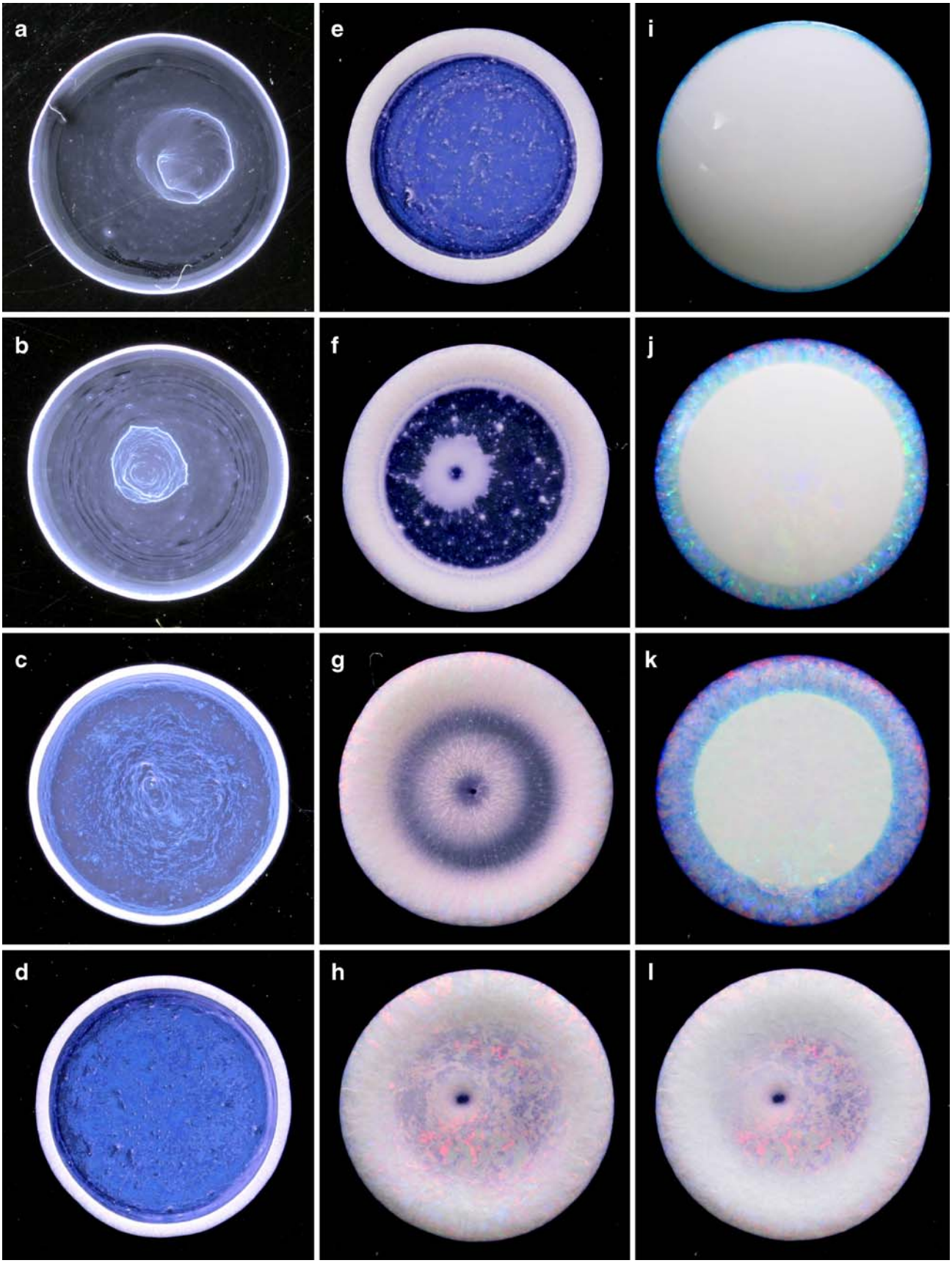

Fig. 6 Drying patterns and change of patterns during dryness of GW8 spheres on a cover glass at 24 °C. **a** ϕ=0.000245, **b** 0.00074, **c** 0.00245, **d** 0.0049, **e** 0.0123, **f** 0.0245, **g** 0.049, **h** 0.074, **i** ϕ=0.074, 35 m after setting, **j** 2 h, 25 m, **k** 3 h, 20 m, **l** 4 h

downward flow of the circular cell convections (see the schematic picture of Fig. 5(a) of [6]). It should be mentioned that the cell convections were not observed for the suspensions of PMMA spheres in this work. Furthermore, the spoke lines formed by the downward flow of spheres were observed clearer than those by upward flow. Secondly, number of the spoke lines was small at the initial stage of the growth of the spoke lines. However, the number increased with time and then decreased, passing the maximum number near the final stage of drying (see also Fig. 4). Thirdly, the round spots appeared at the central side end of the spoke lines, though some of the spots existed without spoke lines and also some of spoke lines without spots. From the authors' experiences on convectional patterns, the authors believe that all the round spots are the *hollows* and not *hills*. Downward convectional flow at the hollows is highly plausible, though the direct observation on the flow direction was impossible in this work.

Figure 2 on GW6 spheres showed also the three observations mentioned above clearly. Figure 3 shows the change in the convectional patterns of GW8 spheres. Here, the number of spoke lines was larger than those shown in Figs. 1 and 2. Findings from first to third mentioned above clearly held, irrespective of sphere size. Figure 4 shows the number of spoke lines as a function of time after the suspensions were set. This figure also clearly demonstrates that the fourth finding in the convectional patterns of PMMA spheres, i.e., the number of spoke lines, increased as sphere size increased. However, the reason for this finding is not always clear.

Drying patterns of PMMA spheres

Figure 5 and 6 show the typical examples of the drying patterns of GW1 and GW8 spheres as a function of the sphere concentration (pictures a to h). These pictures also show the typical examples of the pattern change during the course of dryness of the colloidal crystal suspensions of GW1 and GW8, respectively (from i to j, k, l, and h in Figs. 5 and 6). Several important findings are noted. Firstly, colors of the dried films changed from bluish to pinky and then whitey as the sphere size increased (from GW1 to GW6, GW8, and PM1000). These brilliant iridescent colors, especially for GW1, GW6, and GW8, support the existence of the crystal-like ordering of spheres in the solid film state. Secondly, the broad rings were always formed at the outside edge. Clearly, the width of the broad ring increased sharply as the initial sphere concentration increased. Furthermore, another broad ring was also formed in the central region of the dried film, in addition to the broad rings on a cover glass. As mentioned above, it is highly plausible that the temporal and reversible aggregate formation of the weakly hydrophobic spheres of PMMA takes place. The aggregates must be rather difficult to move toward outside by the convectional flow and accumulate on the central area. It should be noted that the coexistence of the round hill at the central area and the broad ring at the outside region has been reported for the drying patterns of the anisotropically shaped colloidal particles such as bentonites [38] and green tea [10]. Thirdly, the spoke lines, cracks in this work, were observed so often in the broad ring areas and sometimes in the central area too, irrespective of the sphere concentrations. These spoke lines are quite similar to the observations of colloidal silica [33] and poly (styrene) spheres [34]. However, quantitative discussion on the spoke-line number of the PMMA films was difficult in this work. It should be mentioned here that the color change during the course of dryness of PMMA colloidal crystals was significant and beautiful compared with those of other suspensions such as colloidal silica and polystyrene spheres (see especially Fig. 6 from pictures i to j, k, l, and h). Especially, the highly concentrated suspensions of GW1 to GW8 in the liquid state emitted strong iridescent colors. These colors, however, disappeared and became whitey in the dried film in many cases. This will be due to the strong multiple scattering of visible light by the dried

Table 1 Pattern area (S) and drying time (T) of GW1, GW6, GW8, and PM1000 spheres as a function of sphere concentration at 25 °C, 25 °C, 24 °C, and 24 °C, respectively

GW1			GW6			GW8			PM1000		
ϕ	S (mm^2)	T (min)	ϕ	S (mm^2)	T (min)	ϕ	S (mm^2)	T (min)	ϕ	S (mm^2)	T (min)
0.000318	105	–	0.00021	106	275	0.000245	109	280	0.000266	117	290
0.00095	102	270	0.00063	100	275	0.00074	106	280	0.00080	113	290
0.00318	104	270	0.0021	106	275	0.00245	108	280	0.00266	115	290
0.0064	105	270	0.0042	106	275	0.0049	109	280	0.0053	109	270
0.0159	115	270	0.0105	108	275	0.0123	109	280	0.0133	109	270
0.0318	117	255	0.021	113	260	0.0245	113	265	0.0266	117	270
0.064	121	255	0.042	129	250	0.049	119	245	0.053	109	270
0.095	123	240	0.063	133	245	0.074	123	245	0.080	113	235

films. The partial fusion (or coalescence) of the PMMA spheres followed by the partial breaking of the crystal structures and the enhanced multiple scattering may be one of the main reasons for this observation.

The areas (S) covered with the PMMA spheres in the dried film at various initial sphere concentrations are compiled in Table 1. The S values increased when sphere concentration increased especially for small spheres. For PM1000 spheres, S was rather insensitive to ϕ within the experimental errors. The ϕ dependency in S values on a cover glass has been often observed for other suspensions and solutions, including colloidal silica spheres, detergents, and polyelectrolytes in our laboratory [6, 33, 36, 37, 39–41, 45–47]. The main cause for this characteristic concentration dependency of the pattern area has been clarified to be the increased surface activity of the colloidal suspensions at the air–suspension interface. Surface tensions of many kinds of solutions and colloidal suspensions, including polystyrene and colloidal silica spheres, decreased as solute concentration increased [45, 56–58]. The drying time (T) decreased when sphere concentration increased. In other words, T decreased as S increased. This observation has often been

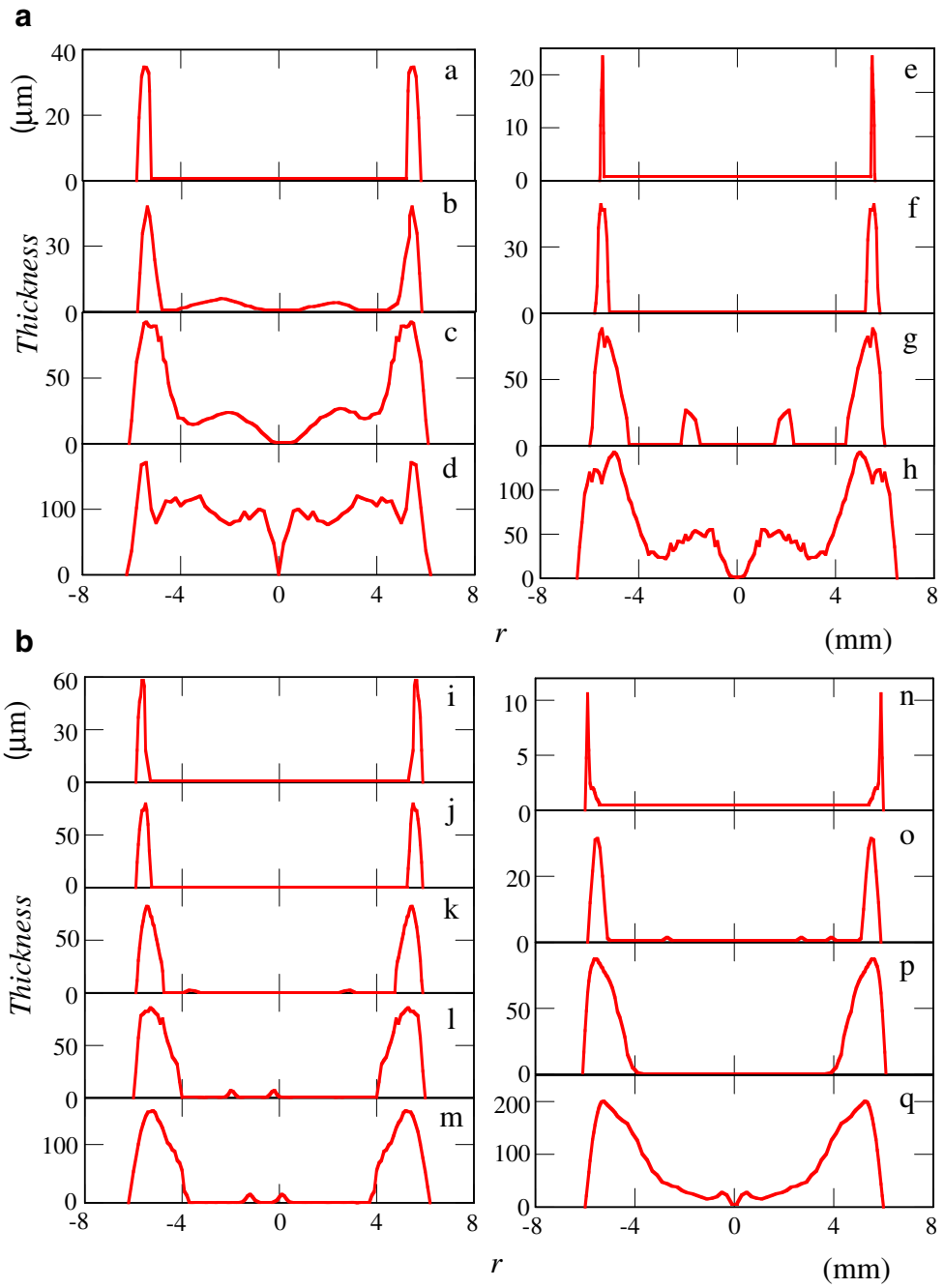

Fig. 7 **a**–**h** Thickness profiles of the dried films of GW1 (**a**–**d**) and GW6 spheres (**e**–**h**) as a function of the distance from the center (r). **a** ϕ=0.00318, **b** 0.0064, **c** 0.0318, **d** 0.095, **e** 0.00063, **f** 0.00420, **g** 0.0210, **h** 0.063. **i**–**q** Thickness profiles of the dried films of GW8 (**i**–**m**) and PM1000 spheres (**n**–**q**) as a function of the distance from the center (r). **i** ϕ=0.00245, **j** 0.0049, **k** 0.0123, **l** 0.0245, **m** 0.074, **n** 0.00080, **o** 0.0053, **p** 0.0266, **q** 0.080

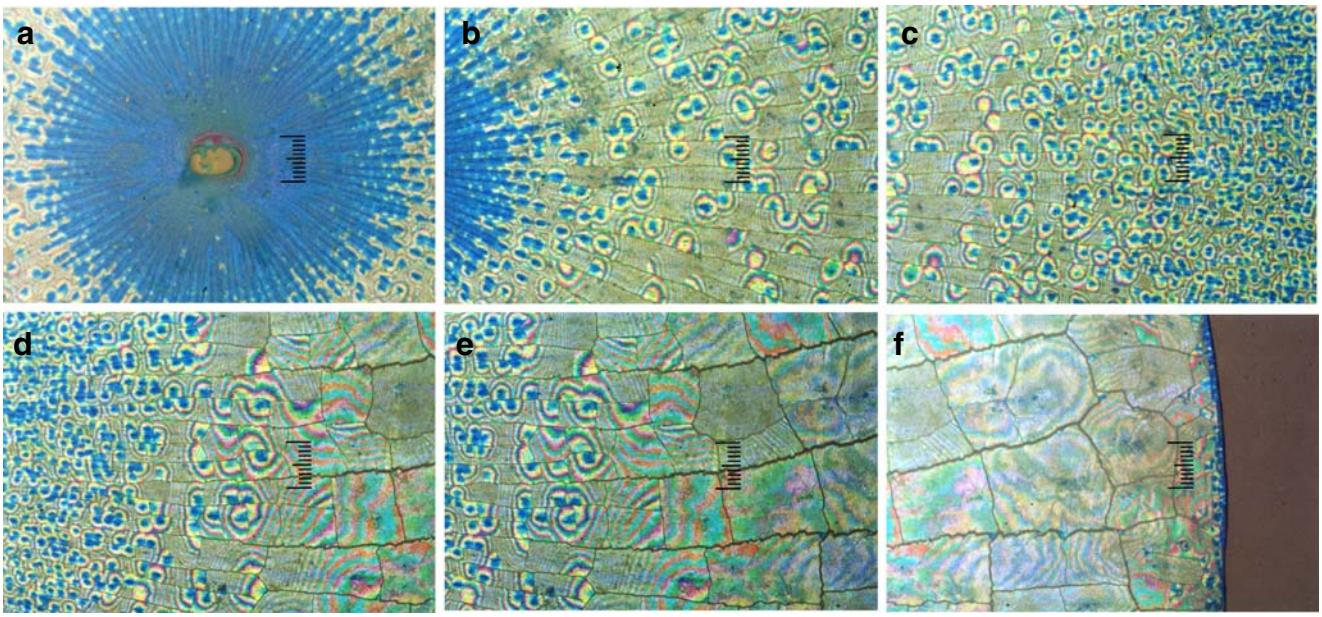

Fig. 8 Microscopic drying patterns of GW6 spheres on a cover glass at 25 °C. ϕ=0.0420, 0.1 ml, dry, from center (**a**) to right edge (**f**), full scale= 200 μm

observed [36, 39, 40, 45] and quite understandable because the drying process is fast when the liquid film is thin even though the area is large.

Figures 7a and b show the thickness profiles of the dried films of GW1, GW6, GW8, and PM1000 spheres at the various initial sphere concentrations. Several findings are clear in the figures. Firstly, the sharp broad rings were formed at the low sphere concentrations irrespective of sphere size. Secondly, the broad ring came to be broad as the sphere concentration increased. Thirdly, the broad ring at the central area developed in addition to the broad ring at the outside edge, with increasing sphere concentration and/or decreasing sphere size.

Figure 8 shows the typical example of the microscopic pictures of GW6 spheres at rather high sphere concentration, ϕ=0.0420, from the central area to the right outside edge of the dried film. The central area shown in panel a is very thin, and the broad ring region is shown in panels e and f. Beautiful colors are due to the Bragg diffraction of light by the crystal-like array of the PMMA spheres in the film. It should be noted here that a large number of the spoke lines (cracks in this work) at the central area were observed, whereas cracks at the broad ring region were few. In other words, the crack number increased as the thickness of the dried film decreased, which is the similar observation reported so often hitherto for colloidal silica and polystyrene spheres [33, 34, 43]. It should be mentioned here that the microscopic drying patterns of GW6 spheres at the central area and at the low sphere concentrations were different from those shown in Fig. 8. The spoke lines were not observed, and the irregular and bumpy blocks were observed instead, which are quite similar to the "Shigaraki Yaki"-like patterns observed previously for Chinese black ink [6]. The basic aspects of the microscopic patterns of the other spheres were similar to Fig. 8, though color changed from bluish to whitey, and the pattern size decreased as sphere size increased. Showing the other microscopic patterns was, however, omitted in this paper to save space.

Acknowledgments Financial support from the Ministry of Education, Culture, Sports, Science and Technology, Japan and Japan Society for the Promotion of Science are greatly acknowledged for Grants-in-Aid for Exploratory Research (17655046) and Scientific Research (B) (18350057 and 19350110-0001). The silica sphere sample, CS82, was a gift from Catalyst & Chemical Ind. Co. (Tokyo) to whom the authors appreciate very much.

References

1. Terada T, Yamamoto R, Watanabe T (1934) Proc Imper Acad Tokyo 10:10
2. Terada T, Yamamoto R, Watanabe T (1934) Sci Paper Inst Phys Chem Res Jpn 27:75
3. Terada T, Yamamoto R (1935) Proc Imper Acad Tokyo 11:214
4. Ball P (1999) The self-made tapestry formation in nature. Oxford Univ Press, Oxford
5. Fischer BJ (2002) Langmuir 18:60
6. Okubo T, Kimura H, Kimura T, Hayakawa F, Shibata T, Kimura K (2005) Colloid Polymer Sci 283:1
7. Okubo T (2006) Colloid Polymer Sci 285:225
8. Okubo T (2006) Colloid Polymer Sci 284:1395
9. Okubo T (2006) Colloid Polymer Sci 284:1191
10. Okubo T (2006) Colloid Polymer Sci 285:331

11. Okubo T, Okamoto J, Tsuchida A (2007) Colloid Polymer Sci 285:967
12. Okubo T (2007) Colloid Polymer Sci 285:1495
13. Vanderhoff JW, Bladford EB, Carrington WK (1973) J Polymer Sci Symp 41:155
14. Nicolis G, Prigogine I (1977) Self-organization in non-equilibrium systems. Wiley, New York
15. Cross MC, Hohenberg PC (1993) Rev Modern Phys 65:851
16. Adachi E, Dimitrov AS, Nagayama K (1995) Langmuir 11:1057
17. Ohara PC, Heath JR, Gelbart WM (1998) Langmuir 14:3418
18. Uno K, Hayashi K, Hayashi T, Ito K, Kitano H (1998) Colloid Polymer Sci 276:810
19. Gelbart WM, Sear RP, Heath JR, Chang S (1999) Faraday Discuss Chem Soc 112:299
20. van Duffel B, Schoonheydt RA, Grim CPM, De Schryver FC (1999) Langmuir 15:957
21. Maenosono S, Dushkin CD, Saita S, Yamaguchi Y (1999) Langmuir 15:957
22. Brock SL, Sanabria M, Suib SL, Urban V, Thiyagarajan P, Potter DI (1999) J Phys Chem 103:7416
23. Nikoobakht B, Wang ZL, El-Sayed MA (2000) J Phys Chem 104:8635
24. Ge G, Brus L (2000) J Phys Chem 104:9573
25. Chen KM, Jiang X, Kimerling LC, Hammond PT (2000) Langmuir 16:7825
26. Lin XM, Jaenger HM, Sorensen CM, Klabunde KJ (2001) J Phys Chem 105:3353
27. Kokkoli E, Zukoski CF (2001) Langmuir 17:369
28. Ung T, Liz-Marzan LM, Mulvaney P (2001) J Phys Chem 105:3441
29. Haw MD, Gilli M, Poon WCK (2002) Langmuir 18:1626
30. Narita T, Beauvais C, Hebrand P, Lequeux F (2004) Eur Phys J E 14:287
31. Tirumkudulu MS, Russel WB (2005) Langmuir 21:4938
32. Shimomura M, Sawadaishi T (2001) Curr Opinion Colloid Interf Sci 6:11
33. Okubo T, Okuda S, Kimura H (2002) Colloid Polymer Sci 280:454
34. Okubo T, Kimura K, Kimura H (2002) Colloid Polymer Sci 280:1001
35. Okubo T, Kanayama S, Ogawa H, Hibino M, Kimura K (2004) Colloid Polymer Sci 282:230
36. Okubo T, Kanayama S, Kimura K (2004) Colloid Polymer Sci 282:486
37. Okubo T, Yamada T, Kimura K, Tsuchida A (2005) Colloid Polymer Sci 283:1007
38. Yamaguchi T, Kimura K, Tsuchida A, Okubo T, Matsumoto M (2005) Colloid Polymer Sci 283:1123
39. Kimura K, Kanayama S, Tsuchida A, Okubo T (2005) Colloid Polymer Sci 283:898
40. Okubo T, Shinoda C, Kimura K, Tsuchida A (2005) Langmuir 21:9889
41. Okubo T, Yamada T, Kimura K, Tsuchida A (2006) Colloid Polymer Sci 284:396
42. Okubo T, Itoh E, Tsuchida A, Kokufuta E (2006) Colloid Polymer Sci 285:339
43. Okubo T, Nozawa M, Tsuchida A (2007) Colloid Polymer Sci 285:827
44. Okubo T, Kimura K, Tsuchida A (2007) Colloids Surfaces 56:201
45. Okubo T, Onoshima D, Tsuchida A (2007) Colloid Polymer Sci 285:999
46. Okubo T, Nakagawa N, Tsuchida A (2007) Colloid Polymer Sci 285:1247
47. Okubo T, Yokota N, Tsuchida A (2007) Colloid Polymer Sci 285:1257
48. Okubo T, Kimura K, Tsuchida A (2008) Colloid Polymer Sci 286:385
49. Okubo T, Kimura K, Tsuchida A (2008) Colloid Polymer Sci. (in press). DOI 10.1007/s00396-007-1808-4
50. Erkseliusa S, Wadso L, Karlsson O (2007) Colloid Polymer Sci 285:1707
51. Palmer HJ (1976) J Fluid Mech 75:487
52. Anderson DM, Davis SH (1995) Phys Fluids 7:248
53. Routh AF, Russel WB (1998) AIChEJ 44:2088
54. Burelbach JP, Bankoff SG, Davis SH (1998) J Fluid Mech 195:463
55. Deegan RD, Bakajin O, Dupont TF, Huber G, Nagel SR, Witten TA (2000) Phys Rev E 62:756
56. Okubo T (1988) J Colloid Interface Sci 125:386
57. Okubo T (1995) J Colloid Interface Sci 171:55
58. Okubo T, Kobayashi K (1998) J Colloid Interface Sci 205:433